OFFICE OF NAVAL RESEARCH

TECHNICAL REPORT

FOR

Grant N00014 91 J 1035

R & T Code 413302S

Technical Report No. 14

Structural Effects in Electron Transfer Reactions: Comparative Interfacial Electrochemical Kinetics for *cis*- versus *trans*-Dioxorhenium(V)(bi)pyridine Oxidation

Xiao Lian Zhang and Joseph T. Hupp*
Dept. of Chemistry
Northwestern University
Evanston, IL 60093

Gerald D. Danzer
Dept. of Chemistry
Carthage College
Kenosha, WI

REPORT DOCUMENTATION PAGE

Form Approved
OMB No. 0704-0188

1. AGENCY USE ONLY (Leave blank)	2. REPORT DATE	3. REPORT TYPE AND DATES COVERED
	May 29, 1993	Technical Report, July 92-July 93

4. TITLE AND SUBTITLE

Structural Effects in Electron Transfer Reactions: Comparative Interfacial Electrochemical Kinetics for cis- vs. trans- Dioxorhenium(V)(bi)pyridine Oxidation

5. FUNDING NUMBERS

G.N00014-91-J-1035

6. AUTHOR(S)

Xiao Lian Zhang, Gerald Danzer and Joseph T. Hupp

7. PERFORMING ORGANIZATION NAME(S) AND ADDRESS(ES)

Department of Chemistry
Northwestern University
2145 Sheridan Road
Evanston, IL 60208

8. PERFORMING ORGANIZATION REPORT NUMBER

14

9. SPONSORING/MONITORING AGENCY NAME(S) AND ADDRESS(ES)

Office of Naval Research
Chemistry Division
800 North Quincy Ave.
Arlington, VA 22217-500

10. SPONSORING/MONITORING AGENCY REPORT NUMBER

11. SUPPLEMENTARY NOTES

12a. DISTRIBUTION AVAILABILITY STATEMENT

12b. DISTRIBUTION CODE

13. ABSTRACT (Maximum 200 words)

Abstract: The comparative interfacial oxidation kinetics of the approximate structural isomers, *trans*-$(O)_2Re^V(py)_2^+$ and *cis*-$(O)_2Re^V(bpy)(py)_2^+$ (py is pyridine, bpy is 2,2'-bipyridine) have been assessed in aqueous solution via conventional cyclic voltammetry at a highly ordered pyrolytic graphite (HOPG) electrode. HOPG was employed because of its known propensity to diminish interfacial electron transfer (ET) rates (by ca. 3 to 4 orders of magnitude) and because of a probable lack of importance of kinetic work terms (diffuse double-layer corrections). Measured rates for the trans complex exceed those for the cis by ca. 8-fold. Expressed as an effective activation free energy ($\Delta G^{\ddagger}$) difference this corresponds to a difference (cis - trans) of ~5 kJ mol^{-1}. The actual vibrational barriers to ET have determined from a combination of published x-ray structural results (trans complex) and new resonance Raman results (cis complex). The values are 0.6 kJ mol^{-1} for the trans oxidation and 4.4 kJ mol^{-1} for the cis oxidation (i.e. close to the barrier differenceinferred from rate measurements). Further analysis shows that the majority of the barrier difference is associated with displacement of a (predominantly) Re-N(bpy) stretching mode found only in the cis system. Differences in metal-oxo displacements (cis > trans) are also implicated.

14. SUBJECT TERMS	15. NUMBER OF PAGES
	24
	16. PRICE CODE
	UL

17. SECURITY CLASSIFICATION OF REPORT	18. SECURITY CLASSIFICATION OF THIS PAGE	19. SECURITY CLASSIFICATION OF ABSTRACT	20. LIMITATION OF ABSTRACT
unclassified	unclassified	unclassified	UL

Introduction

We have been exploring the proton-coupled reductions of various dioxorhenium(V) species [1-3] because of the more general insights they provide into the kinetics and thermodynamics of multielectron transfer processes [4-8]. The rhenium(V) complexes are also amenable, however, to proton-decoupled one-electron oxidation — both optically (via metal-to-ligand charge-transfer excitation; eqs. 1-3)[2,3,9-11] and electrochemically (eqs. 4 and 5)[2,3,9-13].

$$trans\text{-}(O)_2Re^{V}(py)_4^{+} \xrightarrow{h\nu} trans\text{-}(O)_2Re^{VI}(py)_3(p\dot{\bar{y}})^{+} \quad (1)$$

$$cis\text{-}(O)_2Re^{V}(bpy)(py)_2^{+} \xrightarrow{h\nu} cis\text{-}(O)_2Re^{VI}(b\dot{\bar{p}}y)\,(py)_2^{+} \quad (2)$$

$$cis\text{-}(O)_2Re^{V}(bpy)(py)_2^{+} \xrightarrow{h\nu} cis\text{-}(O)_2Re^{VI}(bpy)(py)(p\dot{\bar{y}})^{+} \quad (3)$$

$$trans\text{-}(O)_2Re^{V}(py)_4^{+} \longrightarrow trans\text{-}(O)_2Re^{VI}(py)_4^{2+} + e^{-}(electrode) \quad (4)$$

$$cis\text{-}(O)_2Re^{V}(bpy)(py)_2^{+} \longrightarrow cis\text{-}(O)_2Re^{VI}(bpy)(py)_2^{2+} + e^{-}(electrode) \quad (5)$$

(py=pyridine; bpy=2,2'-bipyridine)

Our prior studies of electron transfer (ET) thermodynamics [1,2] (see also Brewer and Gray [10]) revealed a strong dependence of the Re(VI/V) formal potential on ligand substituent characteristics (most notably, substituent electron donating or withdrawing characteristics). The studies also showed — independent of ligand substituent identity — a strong dependence of E_f on "isomeric" form (i.e.

cis versus trans coordination geometry; see figure 1).* In all cases the cis form was more easily oxidized than the corresponding trans, generally by about 600mV.

The origin of the E_f geometry dependence has been explained in terms of the pertinent d-orbital occupancy and the effects of such occupancy upon metal-oxo bonding [3, 11, 14]. In the trans case, the occupied orbital is d_{xy} (where the z-axis is defined by the dioxorhenium core; see fig. 1). Removal of one of the two available electrons via Re(V) oxidation should have no effect upon the core — a notion confirmed by crystallographic studies which indicate identical rhenium-oxygen bond lengths for Re(VI) vs. Re(V) [10, 15-17]. (Similarly, resonance Raman studies of optical oxidation (eq. 1) show that no detectable change in Re-O bond length accompanies the redox transformation [11].) For the cis form, on the other hand, the (doubly) occupied orbital is a composite of d_{xz} and d_{yz} — which unavoidably interacts (unfavorably) with one or more p π^* (oxo) orbitals. A significant driving force for oxidation ($d^2 \rightarrow d^1$, eqs. 2, 3 and 5), therefore, is diminution of the electronic interference and effective enhancement of the rhenium-oxygen bond order. A corollary is that metal-oxo bond compression should accompany Re(V) oxidation. An x-ray crystal structure for *cis*-$(O)_2Re^{VI}(bpy)(py)_2^{2+}$ has yet to be obtained, so direct evidence has been lacking. Resonance Raman studies (reactions 2 and 3) clearly show, however, that a

---

* Because of the synthetic inaccessibility of the required *cis*-$(O)_2Re(py)_4^+$ and/or *trans*-$(O)_2Re(bpy)(py)_2^+$ species, true structural isomers could not be compared. Note, however, that the approximate isomers, *cis*-$(O)_2Re(bpy)(py)_2^+$ and *trans*-$(O)_2Re(py)_4^+$, differ from each other only by the presence or absence of two aromatic protons and a single inter-ring carbon-carbon bond.

significant rhenium-oxygen bond length change accompanies *optical* oxidation [2,11].

Given the very large thermodynamic and related redox structural differences for *cis*- versus *trans*-dioxorhenium(V) oxidation, we reasoned that large *kinetic* differences should exist as well [11]. More specifically, because metal-oxo bond length changes accompany the cis — but not the trans — oxidation, a much higher vibrational activation barrier ought to accompany the cis transformation (eq. 5). In turn, the rate of the cis reaction would be much less than the trans. Experiments reported here show that an interfacial ET kinetic reactivity difference does exist. Although the difference is smaller than we had initially expected, it is in remarkably good agreement with the predictions of a quantitative multi-mode Franck-Condon barrier analysis. The analysis is based in part on published crystal structures [10,15-17] and in part on new resonance Raman measurements.

2. Experimental

Dioxorhenium complexes were prepared and purified as previously described [8]. Water was purified by passage through a Milli-Q purification system. Reagent grade sulfuric acid was obtained from Aldrich Chemical Company Inc. The sodium salt of trifluoromethanesulfonic acid ($NaCF_3SO_3$) was also purchased in reagent-grade form from Aldrich. Ungraded (mottled surface) samples of highly ordered pyrolytic graphite (HOPG) were obtained as a gift from Dr. Arthur Moore of Praxair in Parma, Ohio. Suitable working electrode surfaces

were obtained simply by cleaving the HOPG samples via the transparent adhesive tape lift method.

Electrochemical measurements (on HOPG) were made by using a Pine Instruments potentiostat and an "inverted drop cell" geometry (ca. 2-3mm dia. drop) as described by McCreery and co-workers[19]. The counter electrode was a platinum wire and the reference was a saturated (NaCl) calomel electrode (s.c.e.). Reference electrode contact with the drop was achieved via a narrow-tip glass capillary. To minimize double-layer effects as well as iR drop effects, fairly concentrated electrolyte solutions were employed (i.e. 0.1M H_2SO_4 + 0.5M $NaCF_3SO_3$). Sample concentrations were typically about 1mM.

Interfacial electron transfer rates were obtained by comparing digitized, experimental cyclic voltammograms to digital simulations generated by the explicit finite difference method (CVSIM program obtained from Prof. D. Gosser, Dept. of Chemistry, CUNY [20,21]) or by Nicholson's method [22]. Comparisons were generally made over a range of sweep rates from roughly 20 to 200 mV/sec. (Above 200 mV/sec, distortions evidently due to uncompensated cell resistance were evident.) In view of the relatively high electrolyte concentration and more importantly, the very low interfacial capacitance (ca. 0.3 $\mu F/cm^2$ [23]), no diffuse double-layer corrections were employed. If corrections had been made, however, they would have tended to increase both rate constants, with a very slightly larger (relative) increase in the trans case (since $E_{pzc} \approx -0.2V$ [23]).

Resonance Raman experiments were carried out essentially as previously described [11]. Prior to analysis, however, the resulting spectra were corrected for both instrument response and sample self absorption.

Results

Electrode Kinetics At conventional electrode surfaces such as glassy carbon, both the *cis*- and *trans*-dioxorhenium complexes exhibit purely reversible (i.e. entirely mass-transport and redox-thermodynamics controlled) voltammetric behavior (see figure 2). This mass-transport "masking" makes it impossible, therefore, to observe ET kinetics differences (at least at conventional C.V. sweeping rates). To overcome this difficulty we have turned to highly ordered pyrolytic graphite as an electrode material. McCreery has shown that HOPG electrodes attenuate interfacial ET rates by ca. 3-4 orders of magnitude [19]. Although a full explanation of the attenuation effect has yet to be presented, it is almost certainly (in our opinion) an electronic coupling effect arising from the effectively two-dimensional nature of the graphitic material. Consistent with this explanation, McCreery finds that ET rates at HOPG/solution interfaces are highly dependent on surface defect density (exponentially faster with higher defect density)[19,23]. Importantly, however, he also finds [23] that with carefully handled, low-defect-density surfaces, *relative* rates vary essentially as expected from classical ET activation barrier considerations [24-26].

We have taken advantage of these observations in our evaluation of the molecular geometry dependence of the interfacial ET reactivity of the

dioxorhenium(V/VI) system. Following McCreery, we used the kinetics of the model redox system, $Fe(CN)_6^{4-/3-}$, as an *in situ* probe of defect density [19,23]. He has shown that when the anodic/cathodic voltammetry peak separation (ΔE_p) for $Fe(CN)_6^{4-/3-}$ exceeds ca. 700mV, an HOPG surface can be regarded as nearly (but not perfectly!) defect free from an electrode kinetics point of view. Only surfaces which yielded relatively large ΔE_p values (for $Fe(CN)_6^{4-/3-}$) were accepted, therefore, for subsequent dioxorhenium studies.

In any case, shown in figure 3 are representative voltammograms for *cis*-$(O)_2Re(bpy)(py)_2^{2+/+}$ and *trans*-$(O)_2Re(py)_4^{2/+}$ at low-defect-density HOPG/aqueous-solution interfaces. Notable observations are: 1) that both exhibit comparatively large anodic/cathodic peak separations, clearly indicating interfacial kinetic control of the voltammetry, but 2) that ΔE_p(cis) exceeds ΔE_p(trans), implying slower kinetics for the former.

While both findings were qualitatively reproducible, we observed significant experiment-to-experiment variations. To facilitate a more quantitative comparison, we chose to normalize the Re(VI/V) rate constants (k_{ET}) to those for $Fe(CN)_6^{4-/3-}$ *measured immediately before, at the same surface location.* The normalization procedure yielded $k_{ET}(cis)/k_{ET}(Fe) = 3$ and $k_{ET}(trans)/k_{ET}(Fe) = 25$, where both estimates represent averages of at least 5 separate experiments and 25 separate rate measurements. The $k_{ET}(trans)/k_{ET}(cis)$ ratio, in turn, is estimated as approximately 8.

Structural Changes and Barrier Effects. From standard ET rate theories [24,25] the contribution of internal modes (or vibrations) to the overall reaction barrier (at $E=E_f$) is a simple sum and product function of vibrational frequencies (ν) and unitless normal coordinate displacements (Δ):

$$\Delta G^{\ddagger}_{vib} = (1/8) \sum_i \nu_i \Delta_i^2 \qquad (6)$$

where the sum is over all modes which suffer displacement during the reaction. We note that physically Δ is equivalent to four times* the number of vibrational levels by which the classical transition state lies above the initially unactivated reactant (for the vibrational mode in question).

Alternatively, for local bonding coordinates, the structure/barrier relationship (again at $E = E_f$) is:

$$\Delta G^{\ddagger}_{vib} = (1/8) \sum_j f_j (\Delta a_j)^2 \qquad (7)$$

where f is a force constant and Δa is a real bond-length displacement having dimensions of distance. In some instances, specific local modes are sufficiently similar to specific normal modes to permit the following transformation:

---

*The factor of four is appropriate when the reactant and product potential energy surfaces are reasonably harmonic and when $\Delta G^\circ = 0$ (i.e. when $E = E_f$).

$$\Delta a = (\Delta^2 h/4\pi \mu \nu b)^{1/2} \quad (8)$$

In eq. 8, h is Planck's constant, μ is the reduced mass, and b is the "bond degeneracy" (e.g. 2 for rhenium-oxygen bonds).

For *trans*-dioxorhenium(V/VI) we have noted that x-ray structural [15-17] and resonance Raman data [11] indicate (equivalently) that Δa_{Re-O} and Δ_{Re-O} are zero. On the other hand, the crystal structures do indicate a displacement of the rhenium-nitrogen bonds upon oxidation (Δa_{Re-N} = - 0.04Å) . Transformation via eq. 8 (with μ=65, ν=205 cm^{-1} and b=4) yields $|\Delta_{Re-N}|$=2. Since no other coordinates are significantly displaced, ΔG_{vib}^{*} (eq. 7) is just 100 cm^{-1} or 1.2 kJ mol^{-1}.

For the cis complex, a rhenium(VI) crystal structure is lacking. The x-ray approach, therefore, is not viable for determining coordinate displacements. Nevertheless, the needed information can still be extracted via a time-dependent analysis of Raman scattering experiments. The time-dependent theory [27,28] and pertinent applications [29-34] have been discussed in detail elsewhere. It may be sufficient to note here, however, that the theory (in its simplest form) leads to the following relationship between enhanced scattering intensities (I) for any two vibrational modes and the associated frequencies and displacements:

$$I_1/I_2 = \Delta_1^2 \nu_1^2/\Delta_2^2 \nu_2^2 \quad (9)$$

Importantly, the displacement information obtained is that which is pertinent to the electronic transition giving rise to intensity enhancement. For strongly allowed transitions, eq. 9 should be valid at resonance, provided that a reasonably

large number of modes is enhanced; at preresonance, it should be valid independent of the number of modes enhanced. Note, however, that eq. 9 provides only *relative* coordinate displacements. The needed absolute scaling is available from:

$$2\sigma^2 = \sum_i \Delta_i^2 \nu_i^2 \qquad (10)$$

where $8\sigma^2$ is the square of the electronic absorption bandwidth at 1/e of the height and where the summation is over all enhanced modes that show significant intensity in the scattering spectrum.

The visible portion of the electronic absorption spectrum for *cis*-$(O)_2Re(bpy)(py)_2^+$ is shown in fig. 4. Two transitions are evident. The longer wavelength absorption is due to rhenium-to-bipyridine charge transfer (eq. 2), while the shorter wavelength absorption is due to rhenium-to-pyridine charge transfer (eq. 3). Resonant excitation near 400nm (see figure) should lead primarily to enhancement of those Raman scattering modes associated with the latter transition. It is important to note that from an electrode kinetics point of view the optical transition (eq. 3) is very similar to the interfacial reaction (eq. 5). The former transfers an electron to a pyridine π^* orbital that is geometrically orthogonal to (and therefore, essentially noninteracting with respect to) the dioxorhenium(VI)bipyridine plane (see fig.1); the latter transfers an electron to an electrode. In any case, in the scattering experiment we observe enhancement of a

number of pyridine based modes, as well as rhenium-oxygen and rhenium-nitrogen (bpy) modes. The former obviously gain intensity via displacement effects associated with pyridine radical anion formation (and are irrelevant, therefore, to our electrochemical investigation). The latter, however, are enhanced because of (optical) metal oxidation. The resulting displacements, therefore, are identically those of interest in the electrode reaction.

Analysis of scattering intensities via eqs. 9 and 10 yields $|\Delta_{Re-O}|=0.7$. With ν_{Re-O} = 906 cm^{-1}, μ = 15 and b = 2, eq. 8 yields $\Delta a_{Re-O} \approx \pm$ 0.04Å, where chemical intuition clearly suggests a negative sign for the displacement. In any case, if we view the reaction as one which effectively increases the order of a pair of multiple oxo-metal bonds by ca. 0.25 each, then the estimated extent of the displacement is certainly reasonable [35]. From eq. 6, the estimated contribution of the dioxo-metal displacements to ΔG_{vib}^{*} is 0.6 kJ mol^{-1} (50cm^{-1}).

The displacement is substantially larger in the Re-N(bpy) mode ($|\Delta| \approx 2.6$) which appears at ν = 341 cm^{-1}. Unlike Re-N(py) and Re-O, this mode is *not* purely metal-ligand stretching in character (see fig. 5). Consequently, the unitless displacement is not straightforwardly related to any one particular bond length change. Nevertheless, if we assume for the moment that ν(341) is entirely Re-N(bpy) stretching in character, then an upper limit estimate for $\Delta a_{Re-N(bpy)}$ can be obtained. On this basis we obtain ±0.05Å, where chemical intuition again would strongly suggest bond *compression* upon oxidation. Independent of the

details of the local coordinate displacements, however, eq. 6 can be used to calculate a barrier contribution of 290 cm^{-1} from ν(341).

Finally, the Re-N(py) coordinate is also a candidate for displacement. Resonant scattering from the rhenium-to-pyridine electronic transition (eq.3), however, provides an inadequate route to the electrochemically relevant displacement parameter, since the observed $\Delta_{Re\text{-}N(py)}$ obviously will also be influenced by $p\dot{\bar{y}}$ formation. A more meaningful estimate can be obtained from resonant scattering from the electronic transition in eq. 2. Recall that here the electron is transferred to a bpy(π^*) orbital which is geometrically orthogonal to the py-Re-py axis (see fig. 1). Analysis of Raman data obtained via excitation at 514 nm yields a unitless displacement of ± 1.0. Conversion to local coordinates yields a metal-nitrogen (pyridine) bond length change of ± 0.02Å, where again the change is very likely negative for Re(V) oxidation. Use of either parameter yields a contribution of 0.3 kJ mol^{-1}(30 cm^{-1}) to ΔG_{vib}^{*}(cis). (Rhenium-to-bipyridine excitation also induces, as expected, a displacement in the Re-O coordinate. Curiously, however, the extent of the displacement is less than half that seen with rhenium-to-pyridine excitation. For the Re-to-bpy transition an important additional consideration is that the transferred electron generates a radical anion ($b\dot{\bar{p}}y$) which is coordinated to Re(VI) via N atoms which are necessarily trans to the oxo ligands (fig. 1). The resulting "trans influence" [36] should act to weaken (and lengthen) both Re-O bonds, thereby offsetting to some extent the

strengthening (and shortening) effects anticipated from the rhenium oxidation-state change. This complicating factor would be absent, of course, if the electron were transferred instead to pyridine.)

Summarizing the structural and classical activation barrier effects, we find: (a) $\Delta G_{vib}^{\ddagger}$(trans) ≈ 0.6 kJ mol^{-1} (50 cm^{-1}), with contributions from only one vibrational mode, and (b) $\Delta G_{vib}^{\ddagger}$(cis) ≈ 4.4 kJ mol^{-1}(370 cm^{-1}), with contributions from three vibrational modes.

Discussion

As suggested in the introduction, and reinforced by the structural investigation, significant differences in cis versus trans ET reactivity were expected based on significant differences in (classical) rhenium-oxygen (and rhenium-nitrogen) bond activation requirements. The observed rate differences, however, are modest. Some insight can be gained by casting the differences in terms of an effective activation barrier difference. Assuming that:

$$k_{ET} = A_{ET}\exp(-\Delta G^{\ddagger}/RT) \qquad (11)$$

then:

$$\ln k_{ET}(\text{trans}) - \ln k_{ET}(\text{cis}) = [\Delta G^{\ddagger}(\text{cis}) - \Delta G^{\ddagger}(\text{trans})]/RT \qquad (12)$$

Based on the kinetics measurements, the effective barrier difference is 5 kJ mol^{-1}, i.e. very slightly more than the difference obtained from the structural studies.

One possible mitigating factor in the rate study is that coordinates for high-frequency modes will suffer displacement (in part) via tunneling. To the extent that tunneling occurs, the full activation barrier is not surmounted, the apparent barrier to ET is diminished, and the ET kinetics are accelerated. An approximate expression for the tunneling-corrected vibrational barrier is [25,37,38]:

$$\Delta G^{\ddagger}_{vib}(corr) = 0.5RT \sum_{i} \Delta_i^2 \tanh(h\nu_i / k_B T) \qquad (13)$$

where k_B is Boltzmann's constant. For the trans reactant (where the barrier consists of a single low-frequency displacement) $\Delta G_{vib}^{\ddagger}(corr)$ is essentially identical to the $\Delta G_{vib}^{\ddagger}$ value obtained from eq. 6. For the cis complex, $\Delta G_{vib}^{\ddagger}(corr)$ is roughly 0.1 kJ mol^{-1} less than the classical vibrational barrier. This translates into an extremely small rate effect: a calculated 5% enhancement in $k_{ET}(cis)$, with virtually all of the enhancement coming from tunneling in the dioxo-rhenium coordinate.

Finally, a comparison of the one-electron oxidation kinetics to the previously reported two-electron reduction kinetics [1] may be instructive. For the two-electron reactions the geometry dependence is much larger (ca. 100-fold rate difference); furthermore it is reversed (i.e. trans is *slower* than cis). For the study described here the relative trans/cis kinetics appear primarily to reflect differences in redox-induced structural changes (Franck-Condon effects). In the reduction reactions, related effects may be operative as well. If so, they are clearly overwhelmed, however, by another factor - namely, "thermodynamic" access to the

intermediate one-electron reduction state. Additionally, there are reactivity effects related to the coupling of ET to proton uptake. These, of course, are absent in the pH-independent oxidation processes.

Conclusions

1. HOPG electrodes can be employed to bring the ordinarily quite fast interfacial kinetics of dioxorhenium(V) oxidation into the range of routine experimental accessibility.

2. Within this range, the kinetics of *cis*-dioxorhenium(V) oxidation are consistently slower than the kinetics of *trans*-dioxorhenium(V) oxidation.

3. Seemingly consistent with kinetics observations, the cis compound suffers a detectable displacement in the symmetric rhenium-oxygen stretching coordinate during ET, but the trans does not. A more quantitative analysis shows, however, that differences in metal-oxo displacement are too small, in a Franck-Condon sense, to account for the rate difference.

4. The cis/trans reactivity difference instead appears to be related chiefly to differences in rhenium-nitrogen displacements. For the cis reaction, these displacements (along with the oxo displacements) can be quantified via a time-dependent analysis of Raman scattering data. The analysis shows that the most important activation barrier component is the symmetrical Re-N(bpy) displacement. This component is present, however, only in the cis oxidation, thereby accounting for the diminished kinetics for cis oxidation in comparison to trans oxidation.

Acknowledgements. We thank the Office of Naval Research for support of this work. JTH also acknowledges support from the Henry and Camille Dreyfus Foundation (Dreyfus Teacher-Scholar Award, 1991-96). We thank Dr. Arthur Moore at Praxair for providing the HOPG samples and Prof. James Kincaid at Marquette University for providing access to his Raman instrumentation.

References

1. L.M. Jones-Skeens, X.L. Zhang, J.T. Hupp, *Inorg.Chem.* 31 (1992), 3879.
2. M.S. Ram, L.M. Jones, H.J. Ward, Y.-H. Wong, C.S. Johnson, P. Subramanian, J.T.Hupp, *Inorg.Chem.* 30 (1991) 2928.
3. M.S. Ram, C.S. Johnson, R.L. Blackbourn, J.T. Hupp, *Inorg.Chem.* 29 (1990) 238.
4. T.J. Meyer, *J.Electrochem.Soc.* 131 (1984) 221c.
5. H.H. Thorp, *J.Chem.Educ.* 69 (1992) 250.
6. M.S. Ram, J.T. Hupp, *J.Phys.Chem.* 94 (1990) 2378.
7. D.T. Pierce, W.E. Geiger 114 (1992) 6063.
8. Heinze, *Angew.Chem.* Int.Ed.Engl. 23(1984)831.
9. J.R. Winkler, H.B. Gray, *Inorg.Chem.* 24 (1985) 346.
10. J.C. Brewer, H.B. Gray, Reprints: Symposium on Selective Catalytic Oxidation of Hydrocarbons, ACS Division of Petroleum Chemistry; American Chemical Society: Washington, D.C. 1990; pp. 187-191.
11. C.S. Johnson, C.S. Mottley, J.T. Hupp, G.I. Danzer, *Inorg.Chem.* 31 (1992) 5143.
12. H.H. Thorp, J. Van Houten, H.B. Gray, *Inorg.Chem.* 28 (1989) 889.
13. D.W. Pipes, T.J. Meyer, *Inorg.Chem.* 29 (1986) 3256.
14. J.C. Dobson, K.J. Takeuchi, D.W. Pipes, D.A. Geselowitz, T.J. Meyer, *Inorg.Chem.* 25 (1986) 2357.

15. J.C. Brewer, H.H. Thorp, K.M. Slagle, G.W. Brudvig, H.B. Gray, *J.Am.Chem.Soc.* 113 (1991) 3171.

16. C. Calvo, N. Krishnamachari, C.J.L. Lock, *J.Cryst.Mol.Struct.* 1 (1971) 161.

17. J.W. Johnson, J.F. Brody, G.B. Ansell, S. Zentz, *Inorg.Chem.* 23 (1984) 2415.

18. M.S. Ram, J.T. Hupp, *Inorg.Chem.* 30 (1991) 130.

19. K.R. Kneton, R.L. McCreery, *Anal.Chem.* 64 (1992) 2518.

20. D.K. Gosser, F.Zhang, *Talanta* 38 (1991) 715.

21. Q. Huang, D.K. Gosser, *Talanta* 39 (1992) 1155.

22. R.S. Nicholson, *Anal.Chem.* 37 (1965) 1355.

23. M.T. McDermott, K. Kneten, R.L. McCreery, *J.Phys.Chem.* 96 (1992) 3124.

24. N. Sutin, *Prog.Inorg.Chem.* 30 (1983) 441.

25. N. Sutin, *Comments Inorg.Chem.* 6 (1987) 209.

26. M.J. Weaver in *Comprehensive Chemical Kinetics*, Vol. 27, R.G. Compton, Ed.; Elsevier: Amsterdam, 1988.

27. E.J. Heller, *Acc.Chem.Res.* 14 (1981) 368.

28. E.J. Heller, R.L. Sundberg, D. Tannor, *J.Phys.Chem.* 86 (1982) 1822.

29. J.I. **Zink,** K.-S.K. Shin in *Advances in Photochemistry*, Vol. 16, D.H. Volman, G.S. Hammond and D.C. Neckers, Eds.; John Wiley and Sons, New York, 1991, pp. 119-214.

30. S.K. Doorn, R.L. Blackbourn, C.S. Johnson, J.T. Hupp, *Electrochim.Acta* 36 (1991) 1775.

31. R.L. Blackbourn, S.K. Doorn, J.A. Roberts, J.T. Hupp, *Langmuir* 5 (1989) 696.

32. S.K. Doorn, J.T. Hupp, *J.Am.Chem.Soc.* 111 (1989) 4704.

33. R.L. Blackbourn, C.S. Johnson, J.T. Hupp, *J.Am.Chem.Soc.* 113 (1991) 1060.

34. F. Markel, N.S. Ferris, I.R. Gould, A.B. Myers, *J.Am.Chem.Soc.* 114 (1992) 6208.

35. W.A. Nugent, J.M. Mayer, *Metal-Ligand Multiple Bonds;* John Wiley and Sons: New York, 1988.

36. F.A. Cotton, G. Wilkinson, *Advanced Inorganic Chemistry*, 5th edition, Wiley Interscience, New York, 1988, p. 300.

37. B.S. Brunschwig, J. Logan, M.D. Newton, N. Sutin, *J.Am.Chem.Soc.* 102 (1980) 5798.

38. T. Holstein, *Philos Mag.* 37 (1978) 49.

Figure Captions

1. Chemical structures of *trans*-$(O)_2Re(py)_4^+$ (top) and *cis*-$(O)_2Re(bpy)(py)_2^+$ (bottom).

2. Cyclic voltammograms (200 mV/sec) at glassy carbon in aq. 0.1 M H_2SO_4 + 0.5 M $NaCF_3SO_3$, for (a) *cis*-$(O)_2Re(bpy)(py)_2^+$, and (b) *trans*-$(O)_2Re(py)_4^+$.

3. Cyclic voltammograms (200 mV/sec) at HOPG in aq. 0.1 M H_2SO_4 + 0.5 M $NaCF_3SO_3$, for (a) *cis*-$(O)_2Re(bpy)(py)_2^+$, and (b) *trans*-$(O)_2Re(py)_4^+$.

4. Electronic absorption spectrum for *cis*-$(O)_2Re(bpy)(py)_2^+$.

5. Normal coordinate motion for ν(341).

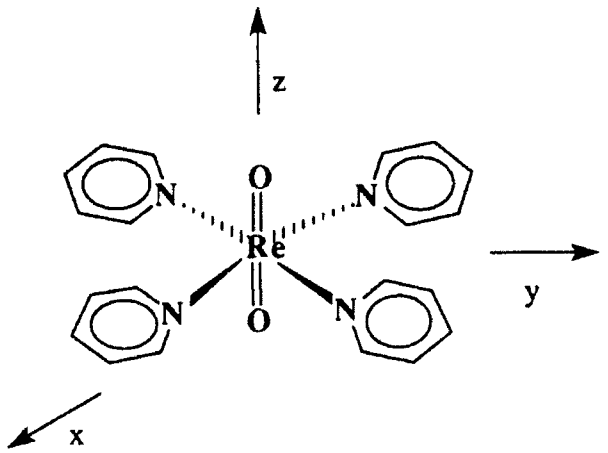
z
O
N
N
Re
y
N
N
O
x

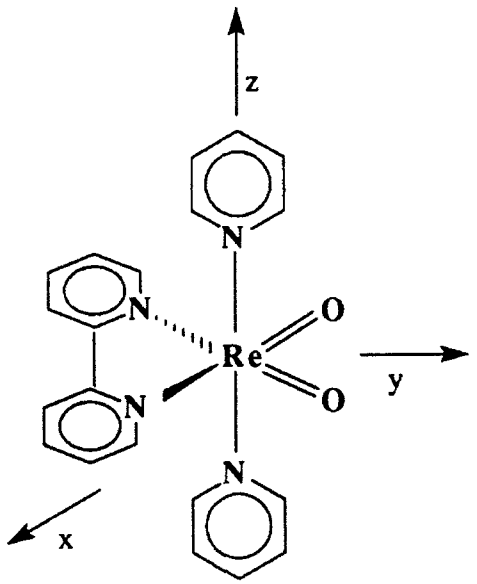
z
N
N
O
Re
y
N
O
N
x

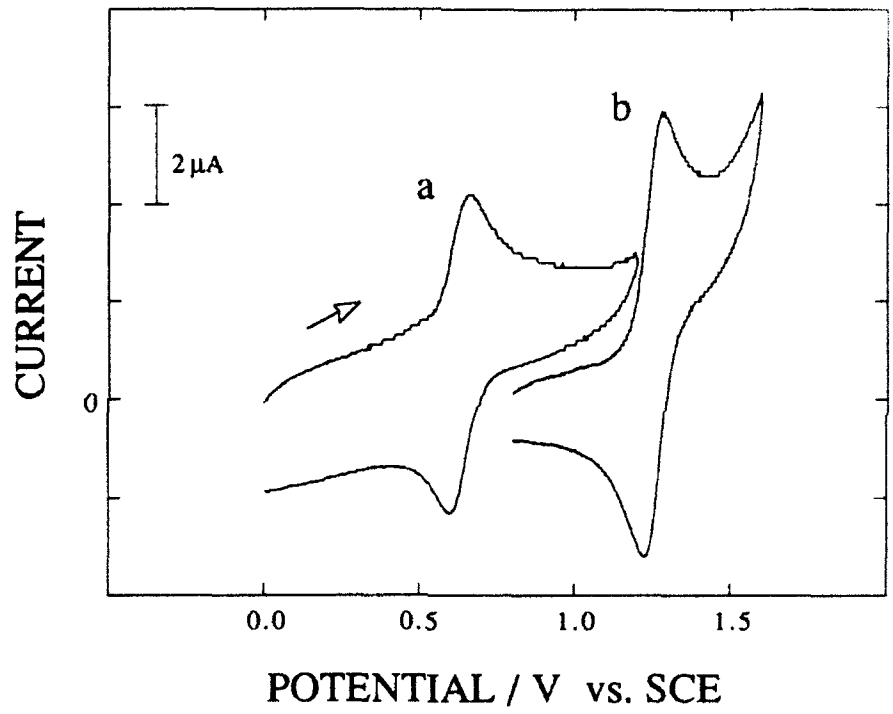
2 µA
a
b
CURRENT
0
0.0
0.5
1.0
1.5
POTENTIAL / V vs. SCE

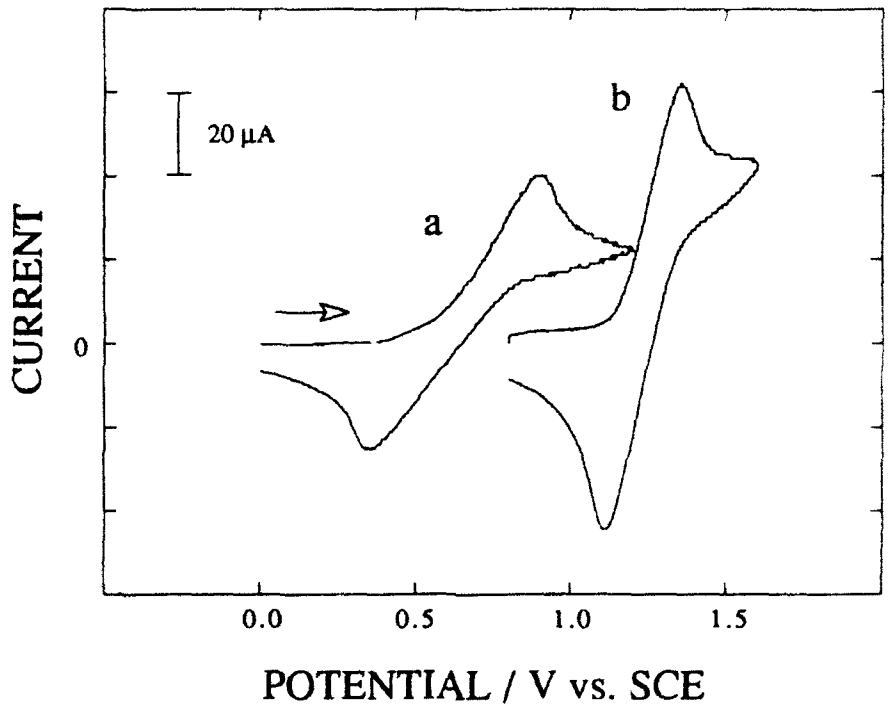
20 µA
a
b
CURRENT
0
0.0
0.5
1.0
1.5
POTENTIAL / V vs. SCE

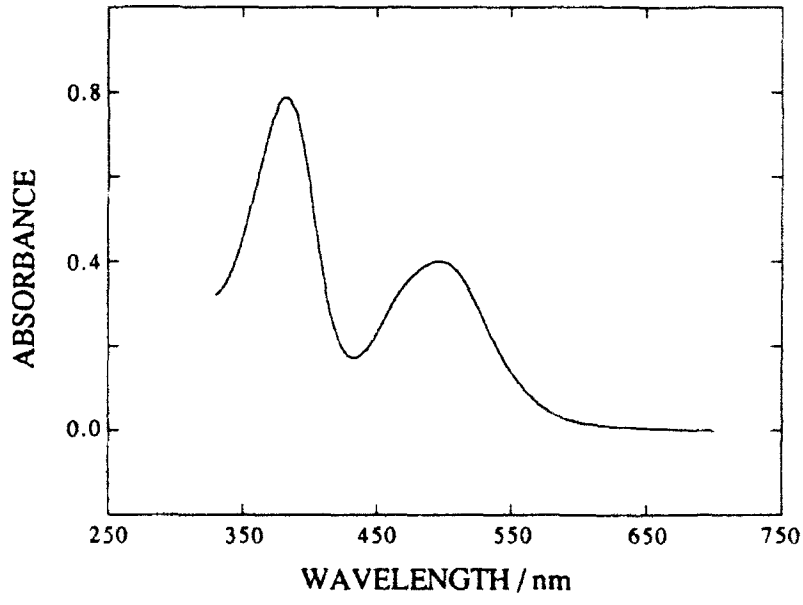
0.8
0.4
0.0
ABSORBANCE
250
350
450
550
650
750
WAVELENGTH / nm